X-ray Spectroscopy at NIST NSLS Beamlines: Recent Upgrades, Scientific Results, and Future Plans

Joseph C. Woicik

National Institute of Standards and Technology

NIST

- *Three x-ray beamlines at NSLS for materials' science research spanning entire periodic table:*
  - U7A
  - X24A
  - X23A2

- *Transition to NSLS-II:*
  - *XAFS and XRD (3 pole wiggler)*
  - *NEXAFS, XPS, and Microscopy (soft and tender canted undulator pair)*

NIST NSLS-II Spectroscopy Beamline Suite: Spectroscopy Soft Tender(SST) and Beamline Materials Measurement(BMM)

Beamline Suite Scientific Mission: *Establish structure function relationships in advanced materials, often at the nanoscale, to accelerate the development of new materials into devices and systems with advanced functionality for promoting innovation and enhancing US industrial competitiveness.*

NIST NSLS-II SST - based on two canted undulator sources;
(1) soft x-rays (100 eV to 2.2 keV) and (2) tender x-rays (1 keV to 7.5 keV).

- ✓ ***6 unique world class NEXAFS/XPS experimental stations*** *(2 full field microscopes, 2 automated high-throughput stations, and 2 insitu high pressure stations).*
- ✓ ***XPS and NEXAFS measurements on the same sample:*** *complete, non-destructive, depth selective measurement of electronic structure, chemistry, and bond orientation.*
- ✓ ***Continuous selection of X-rays from 100 eV to 7.5 keV (at a common focal point)*** *in a single experiment (unique capability, enhancing depth selectivity in XPS; i.e. in Hard X-ray Photoelectron Spectroscopy - HAXPES).*

> *Synchrotron based X-ray Photoelectron Spectroscopy (XPS) and Near Edge X-ray Absorption Fine Structure (NEXAFS) spectroscopy are complementary techniques, probing occupied and unoccupied density of electronic states respectively.*

NIST NSLS-II BMM - 4.5 keV to 35 keV for XAFS and diffraction - 3 pole wiggler

Advanced Synchrotron Measurement Method Development

Soft and Tender Beams Together – 100 eV to 7.5 keV

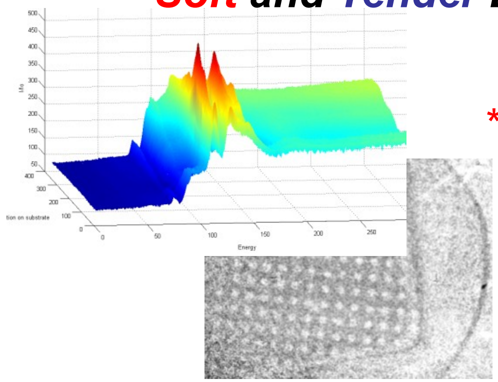

***Soft X-ray NEXAFS microscope**
- SBIR Phase 3 ARRA funded
- under development at NSLS
- micron scale resolution
- 20x20 mm area

Existing U7A NEXAFS/XPS Endstation
- high throughput(x10 NSLS) / insitu
- world class detectors

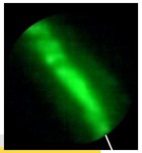

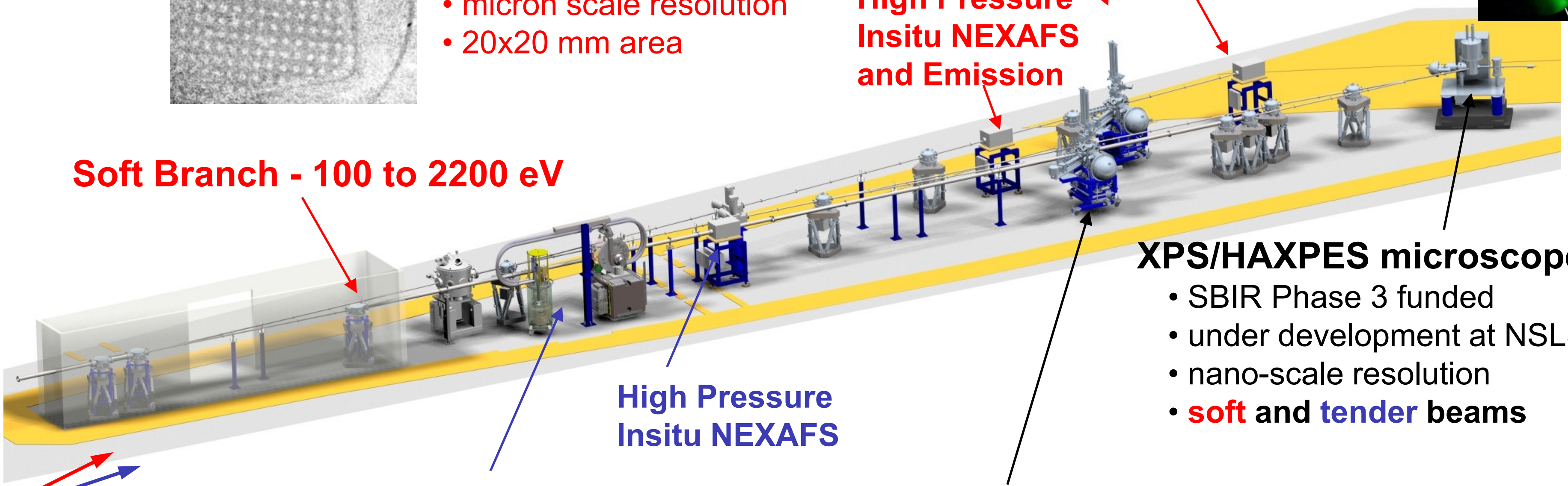

High Pressure Insitu NEXAFS and Emission

*

Soft Branch - 100 to 2200 eV

High Pressure Insitu NEXAFS

Tender Branch - 1 to 7.5 keV

XPS/HAXPES microscope
- SBIR Phase 3 funded
- under development at NSLS
- nano-scale resolution
- **soft** and **tender** beams

NSLS-II
Canted Undulator Pair

Existing X24A HAXPES/NEXAFS Endstation
- high throughput (10x NSLS) / insitu
- world class detectors
- **soft** and **tender** beams

"NIST NSLS-II Spectroscopy Beamline Optical Plan for Soft and Tender X-ray Spectroscopy and Microscopy (100 eV to 7.5 keV)"
R. Reininger, J.C. Woicik, S.L. Hulbert, D.A. Fischer, Nucl. Instr. and Meth. A, doi:10.1016/j.nima.2010.11.172, (2010).

X24A Upgrade

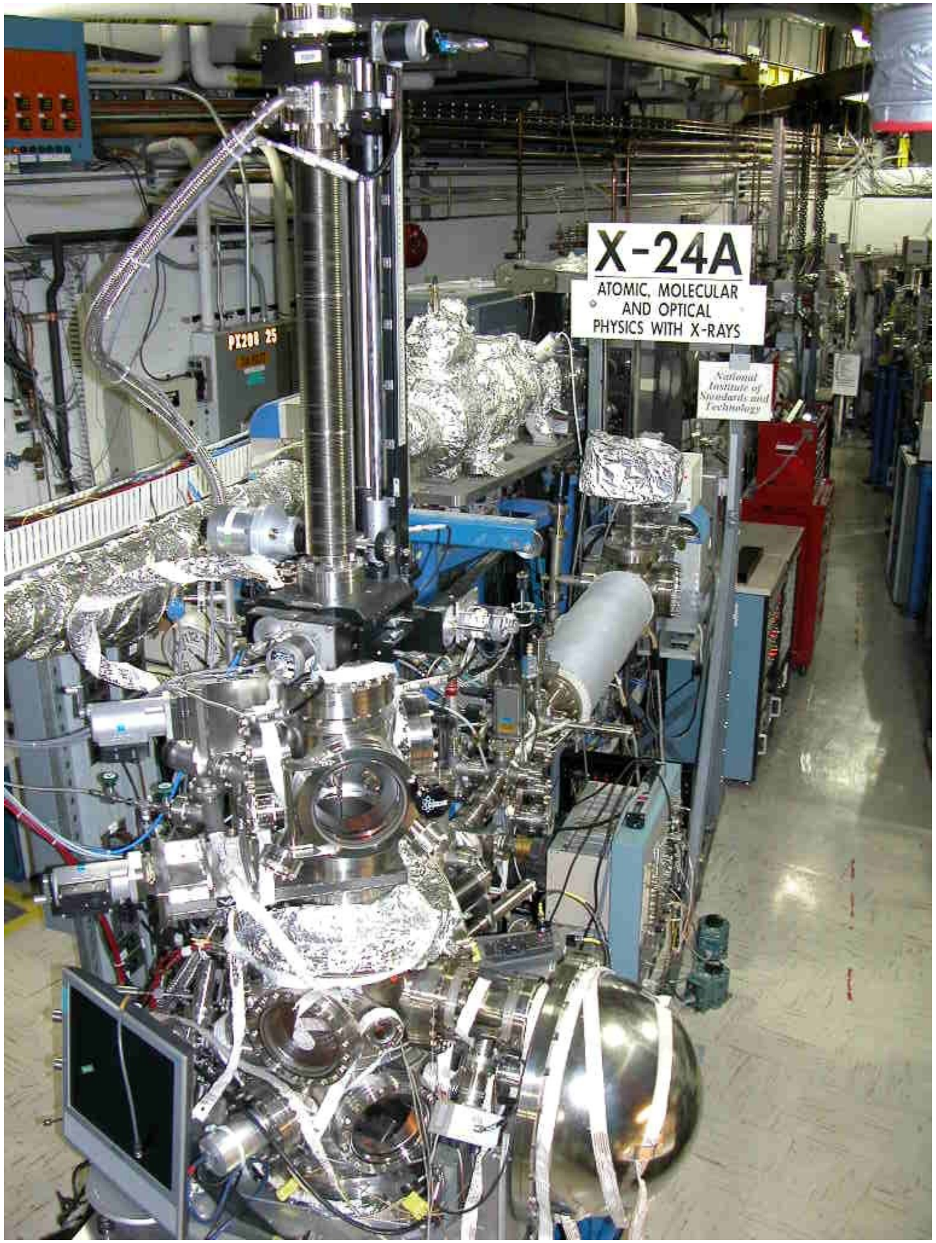

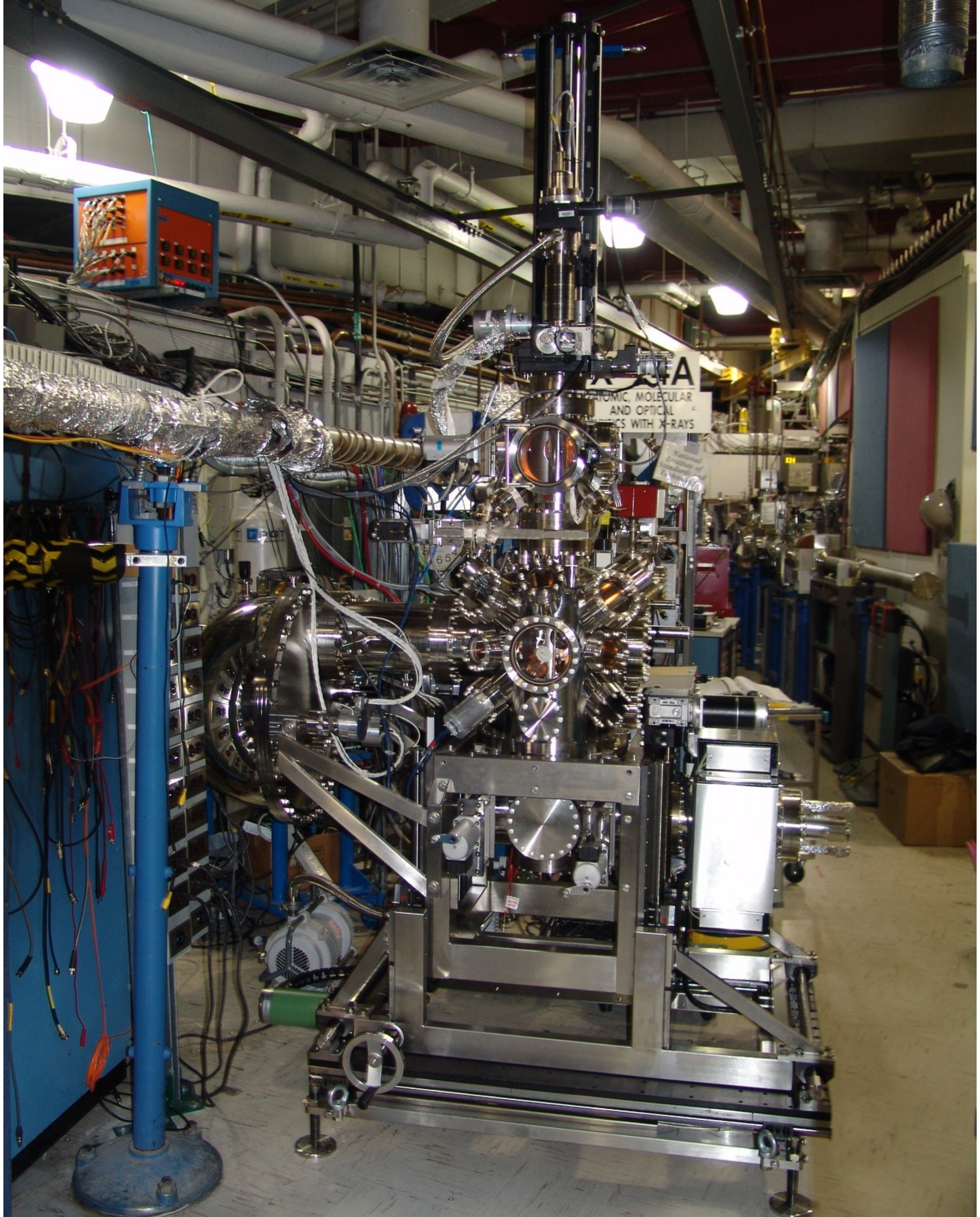
MOLECULAR
AND OPTICAL
WITH X-RAYS

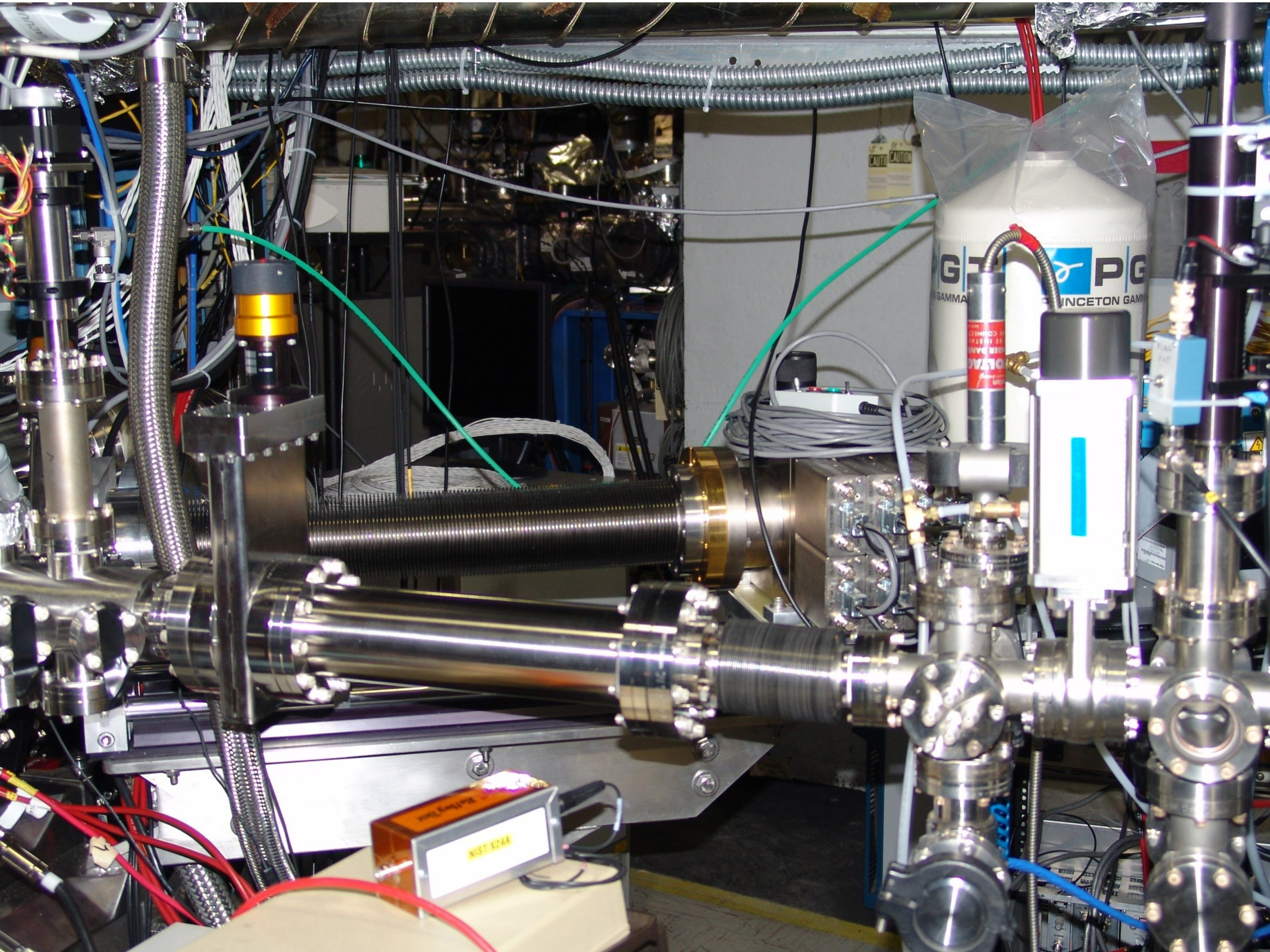
CAUTION

Triple Axis Feedback (θ, χ, mirror)

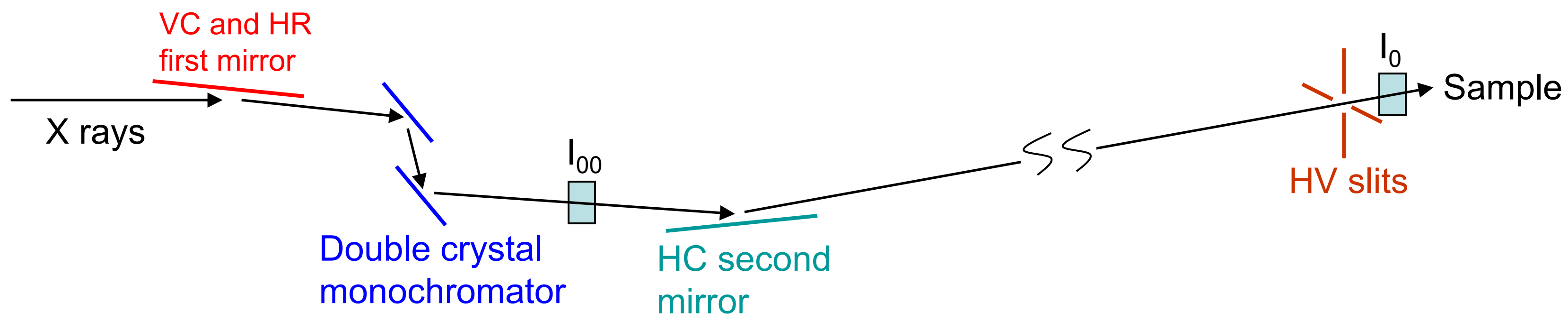

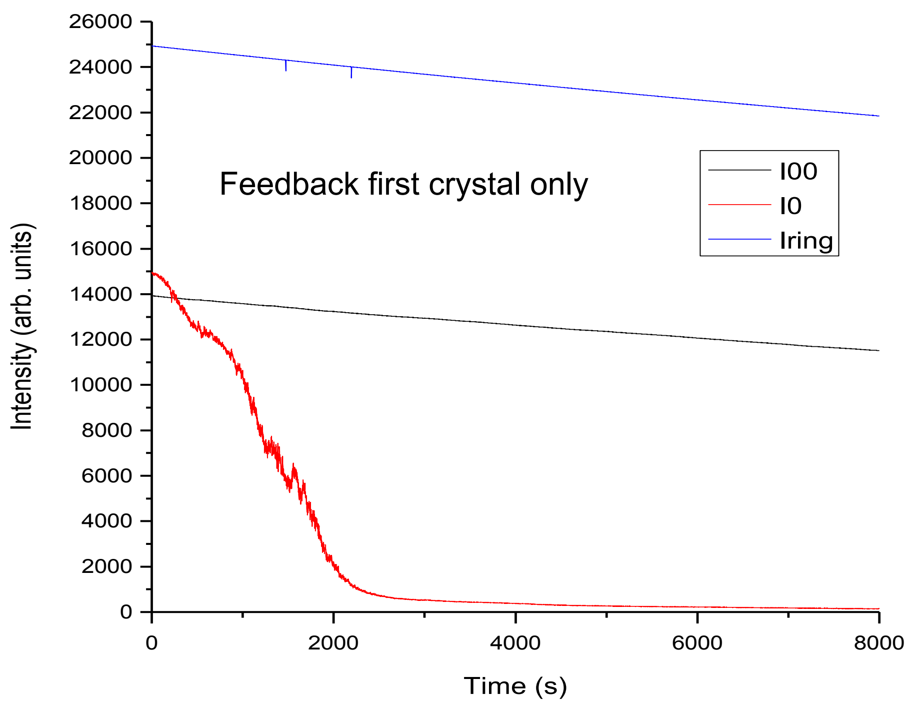

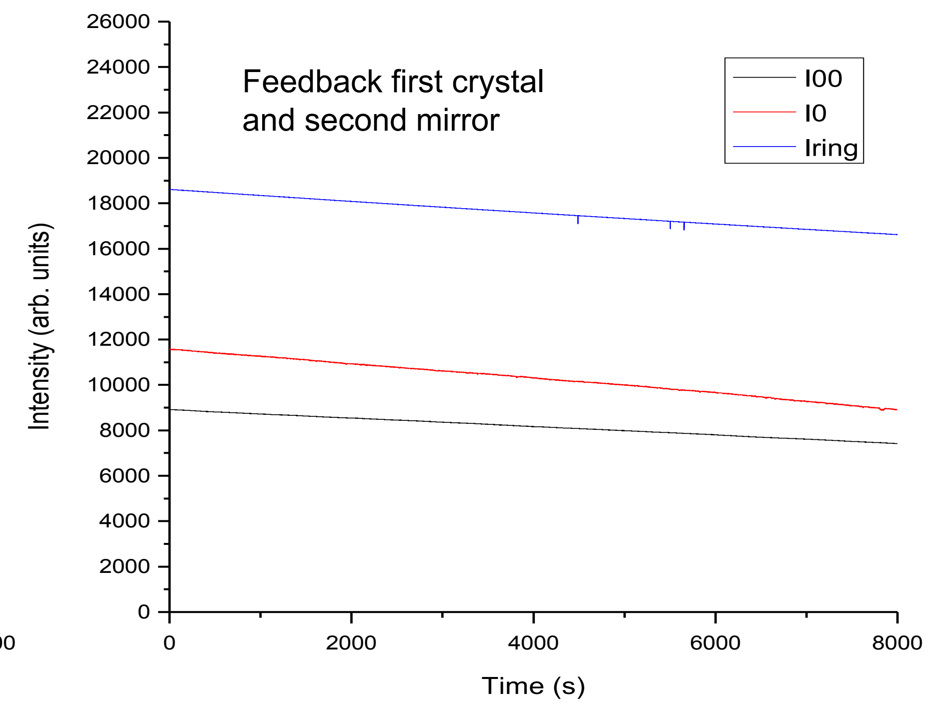

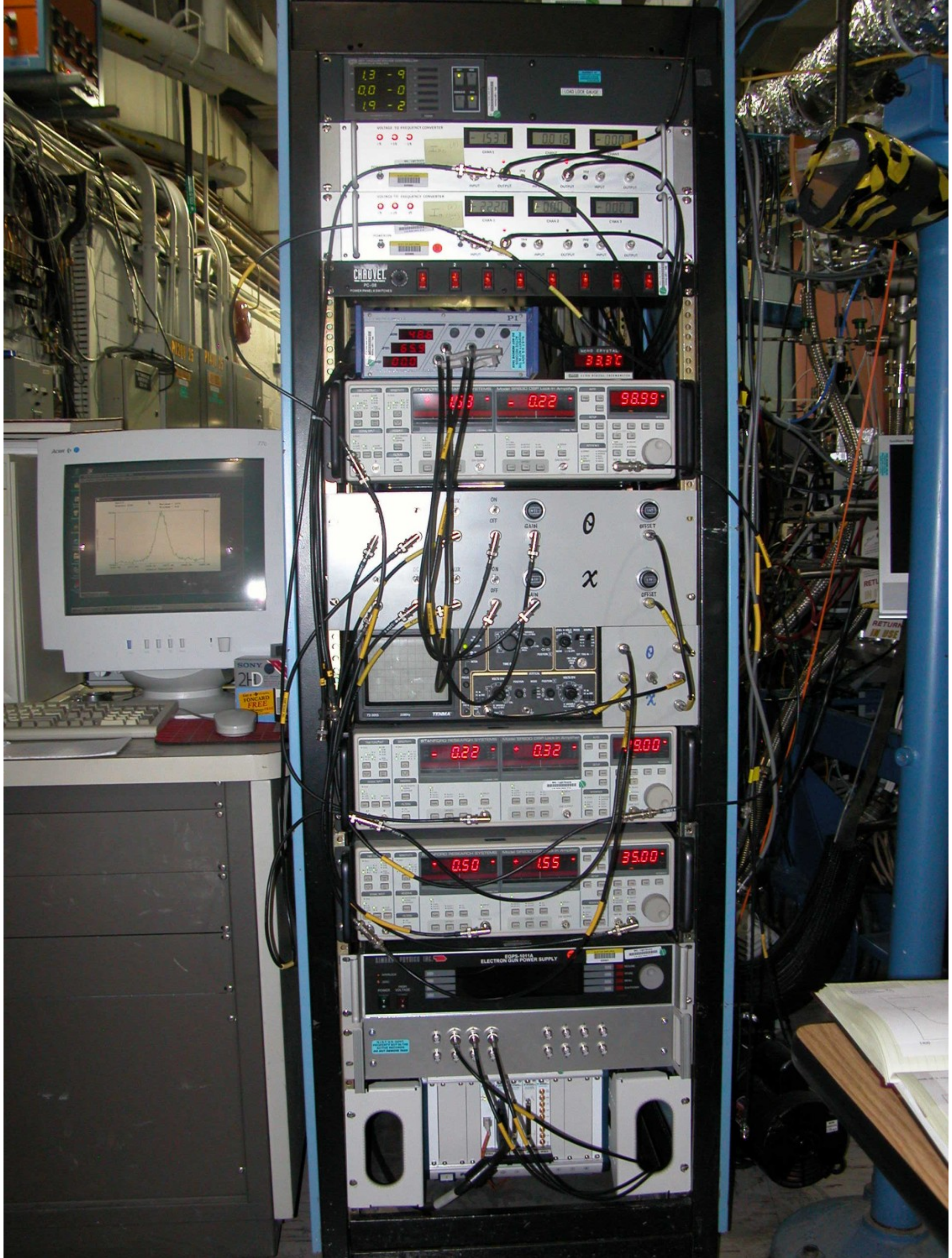

GAIN
OFFSET
ELECTRON GUN POWER SUPPLY

Ag Valence Band

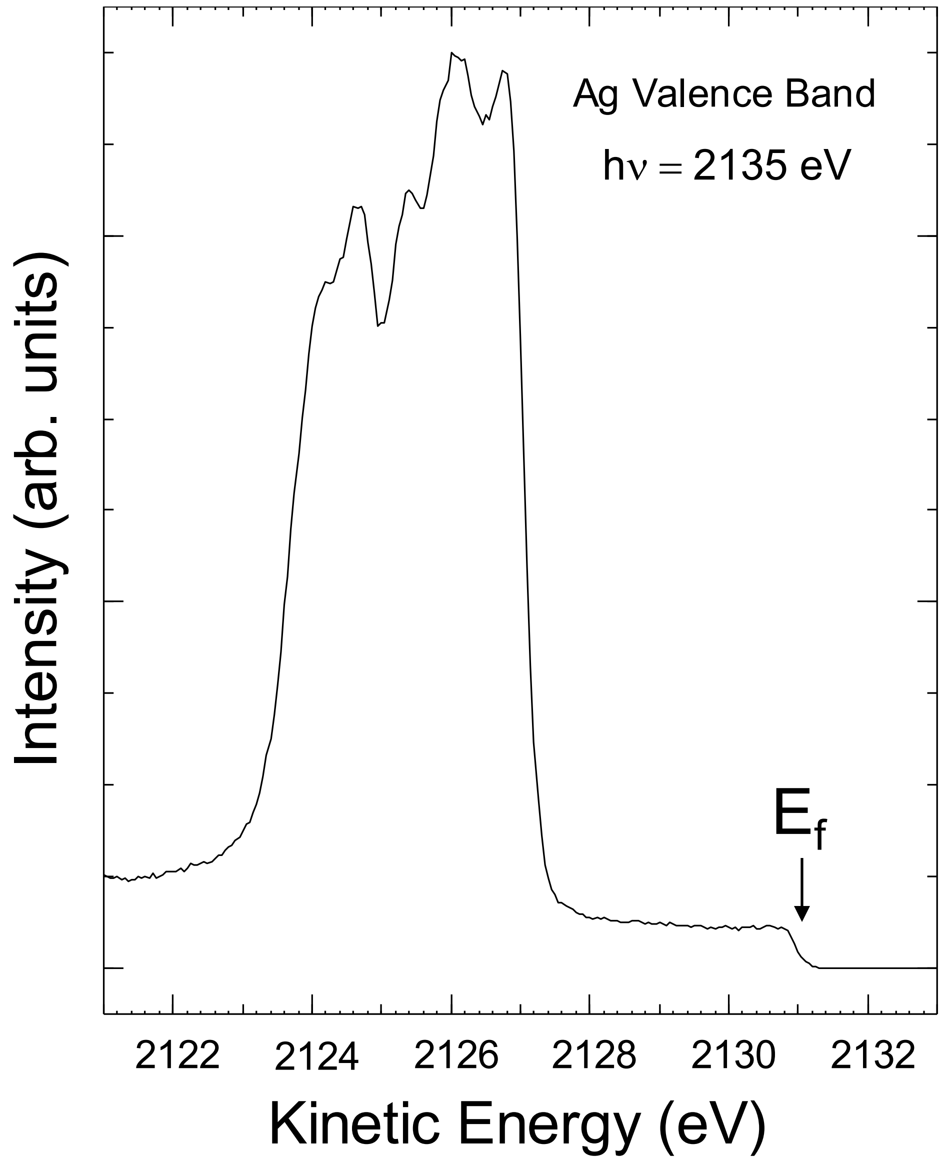

Fermi Foot

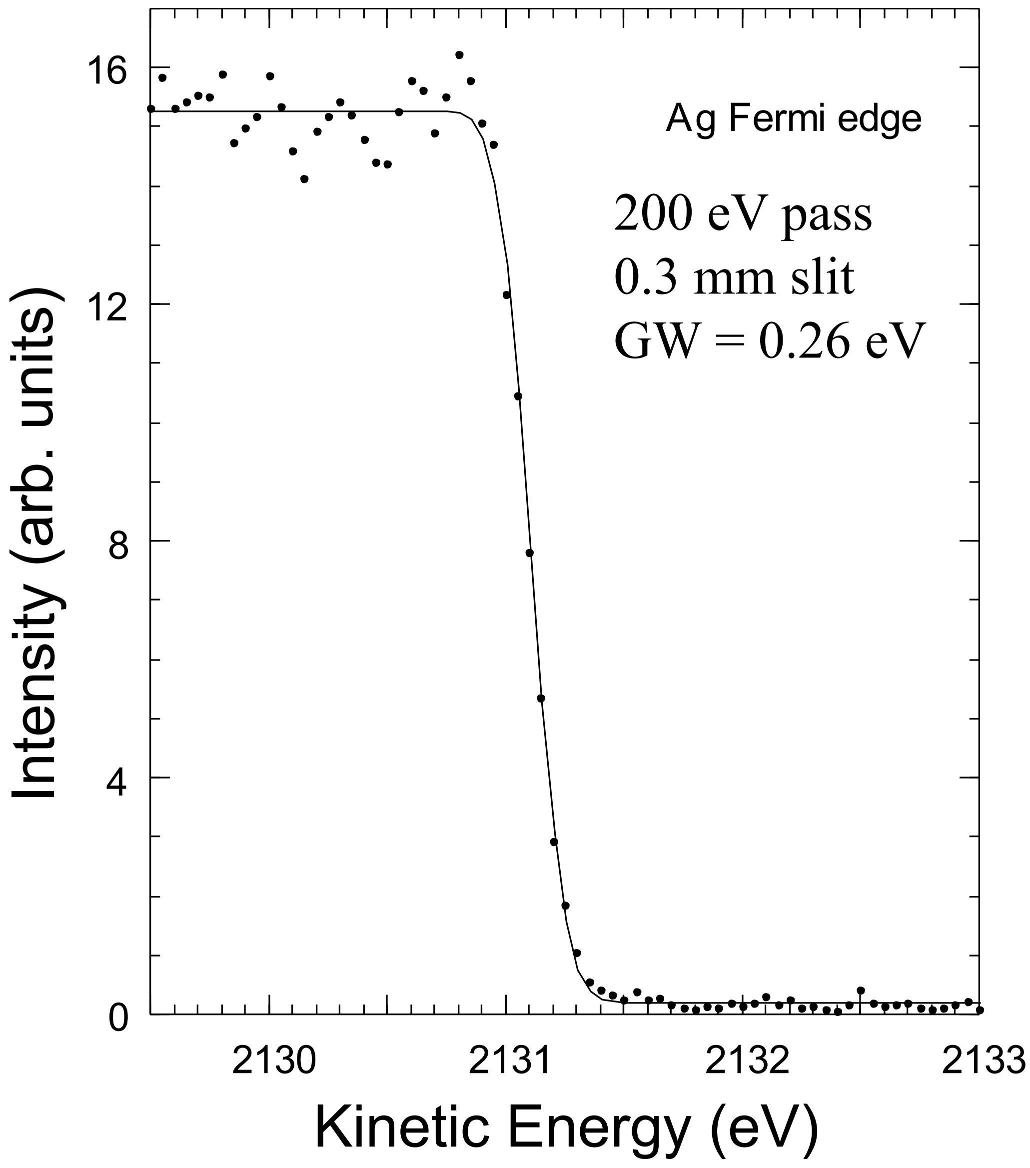

No spectrometer broadening!

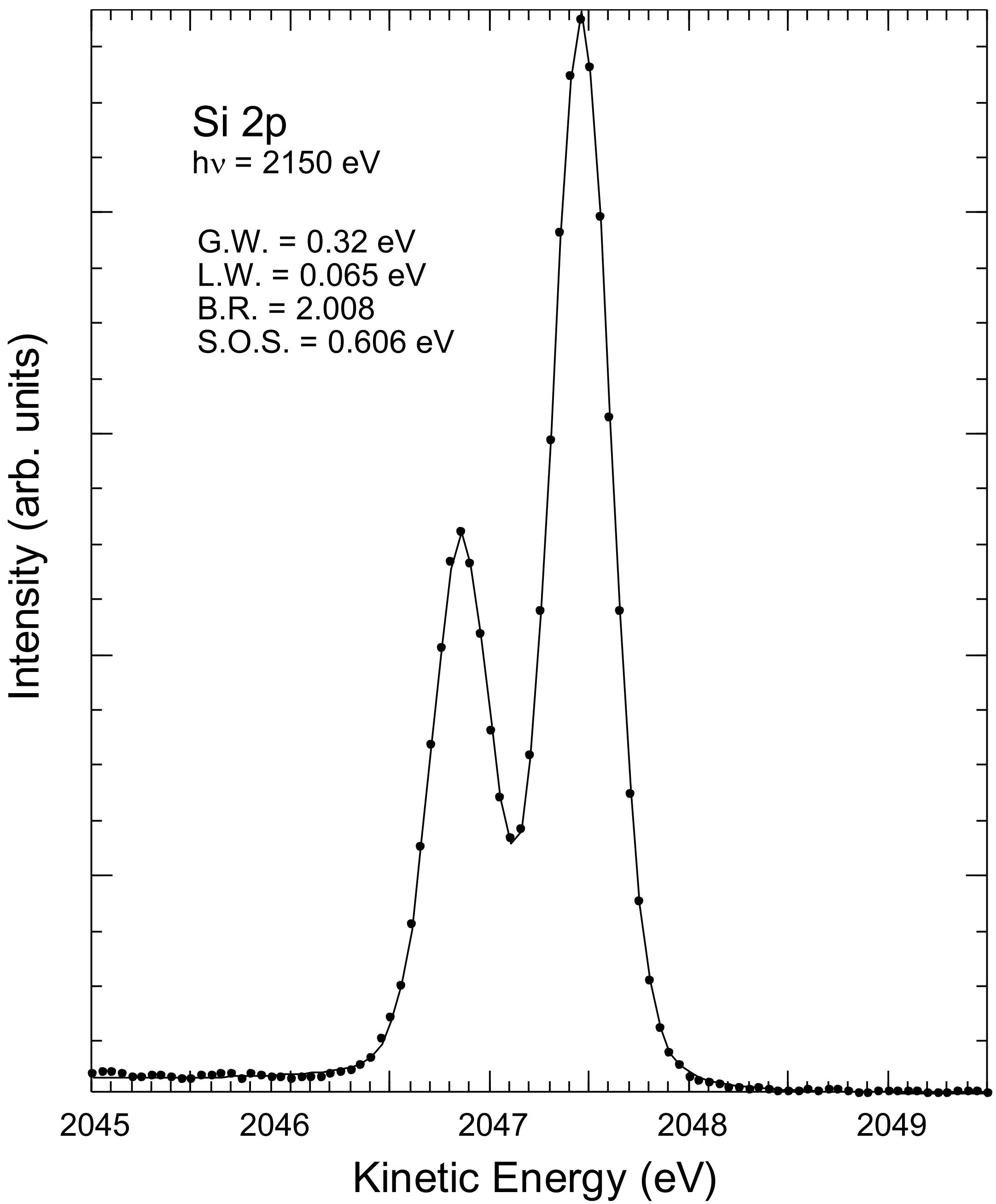

Si 2p
hν = 2150 eV
G.W. = 0.32 eV
L.W. = 0.065 eV
B.R. = 2.008
S.O.S. = 0.606 eV
Intensity (arb. units)
2045
2046
2047
2048
2049
Kinetic Energy (eV)

Introduction

Heterointegration of III-V materials enables advanced SOC

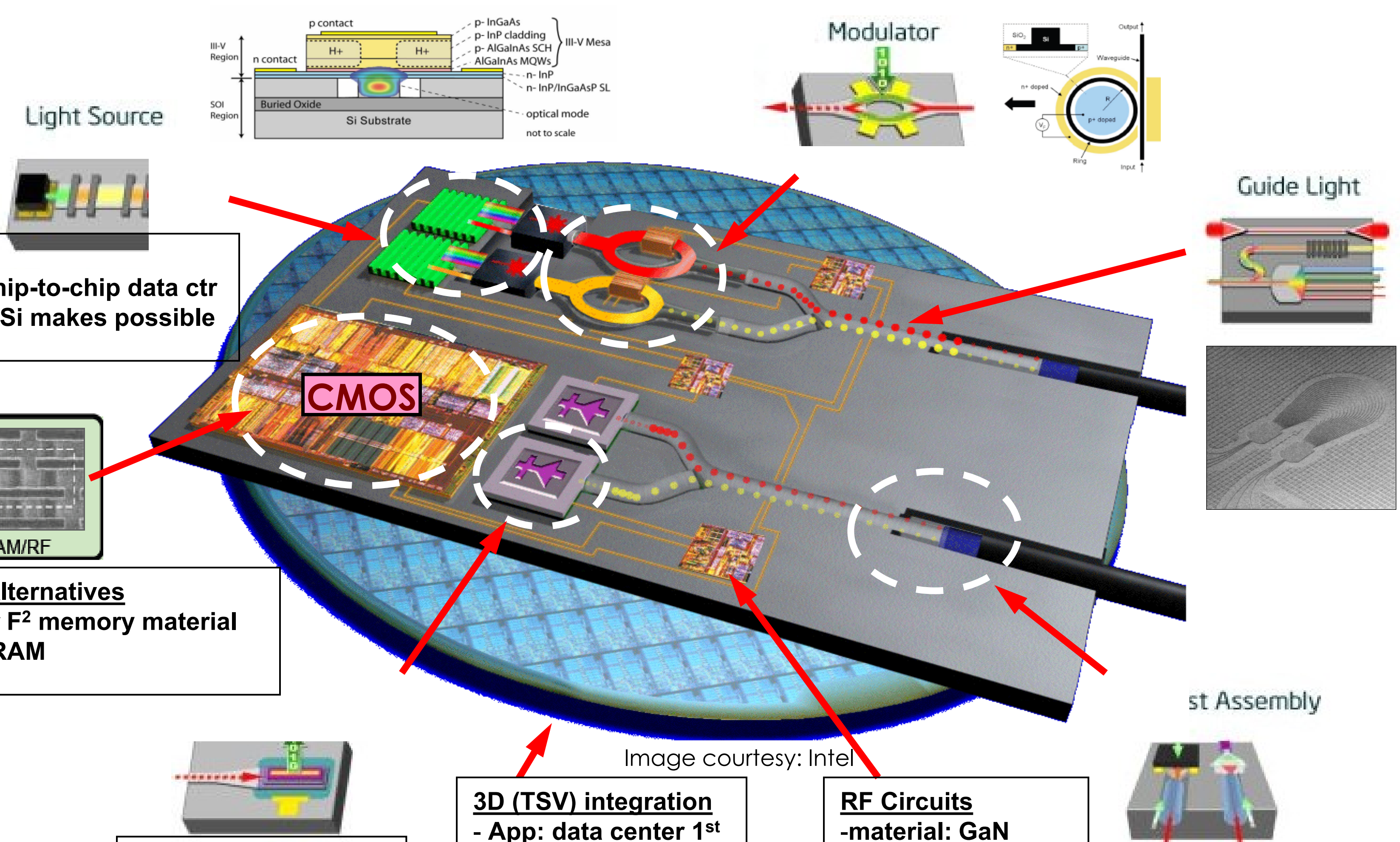

Laser
-App: Chip-to-chip data ctr
-III-V on Si makes possible

SRAM Alternatives
-Smaller F^2 memory material
-STT, RRAM

Photodetector
- App: data center 1st
- Ge epi

3D (TSV) integration
- App: data center 1st
- photons thru TSV

RF Circuits
-material: GaN
- app: phone, tablet

SEMATECH Data

Original analyzer

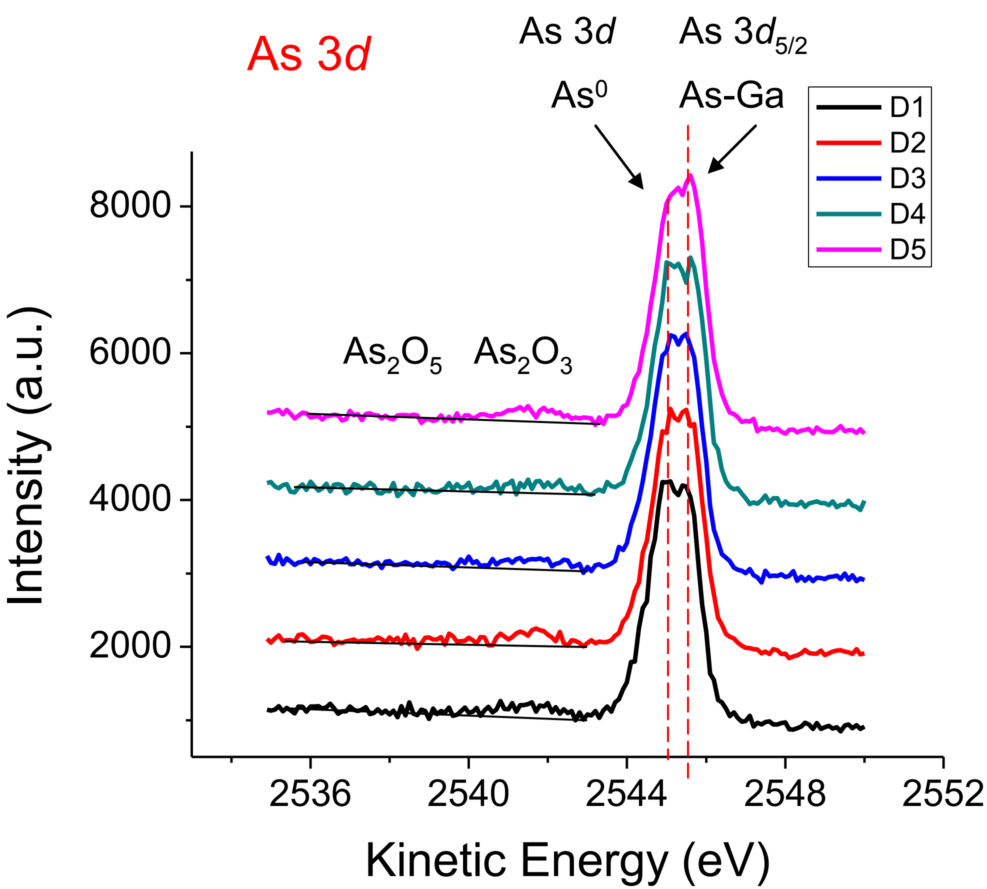

New analyzer

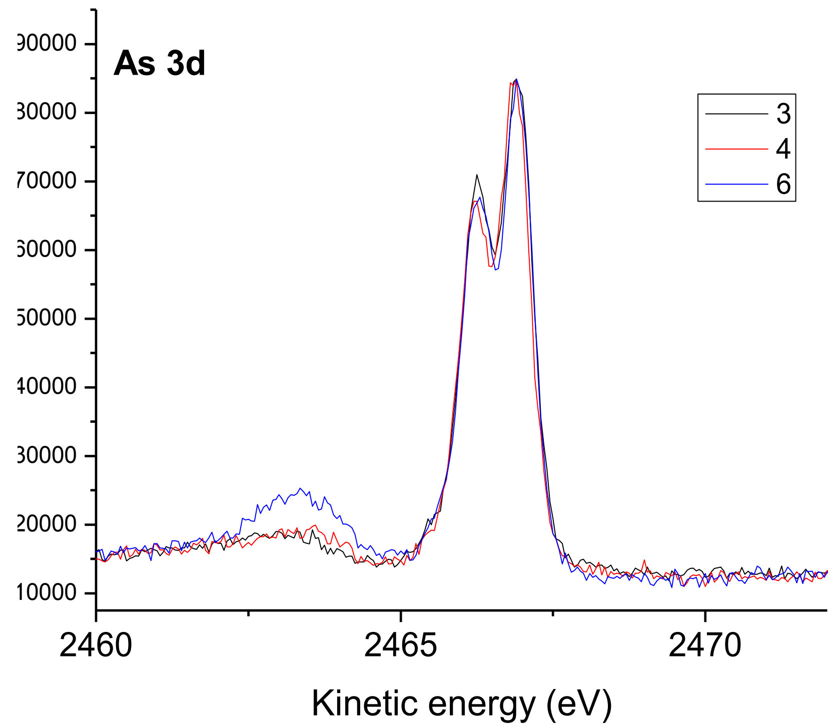

X24A: Talks/Posters

- ***High-K InGaAs interface oxidation control characterization by HAXPES:*** Patrick Lysaght (SEMATECH)
- ***HAXPES studies of oxides and electronic interfaces at NIST beamline X24A:*** Abdul Rumaiz (Brookhaven National Laboratory)
- ***Activation of erbium films for hydrogen storage:*** Michael Brumback (Sandia National Laboratory)
- ***HAXPES characterization of high-K dielectric metal oxide semiconductor structures on InGaAs substrates:*** Gregory Hughes (Dublin City University)
- ***Chemical profiling with photoemission: A comparison between angle-resolved XPS and high-energy photoemission on full gate stacks:*** Christopher Adelmann (IMEC)
- ***Resonant KLL Auger Phenomenon $SrTiO_3$:*** Joseph Woicik (NIST)

$LaCoO_3$ Thin Films

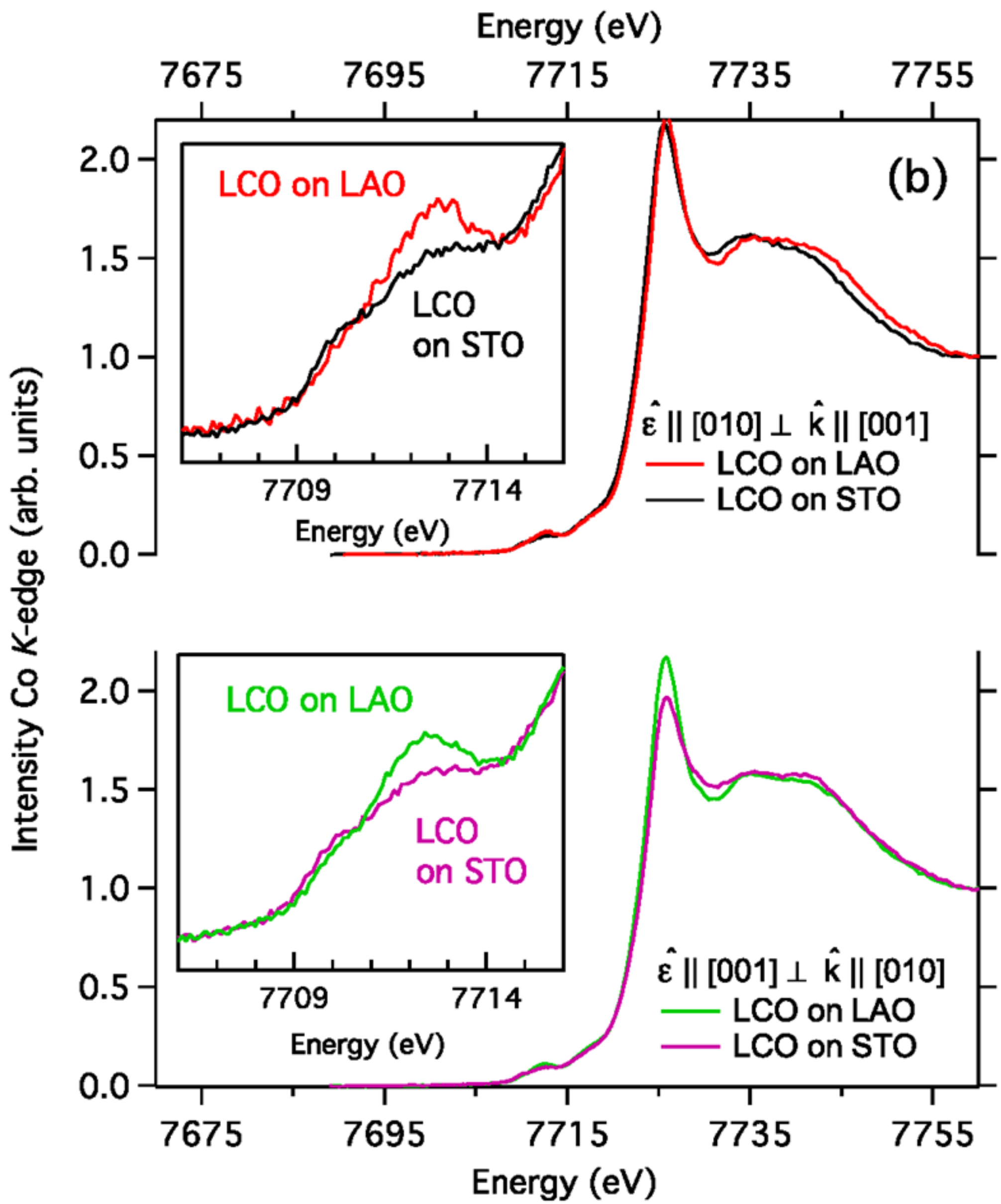

XAFS

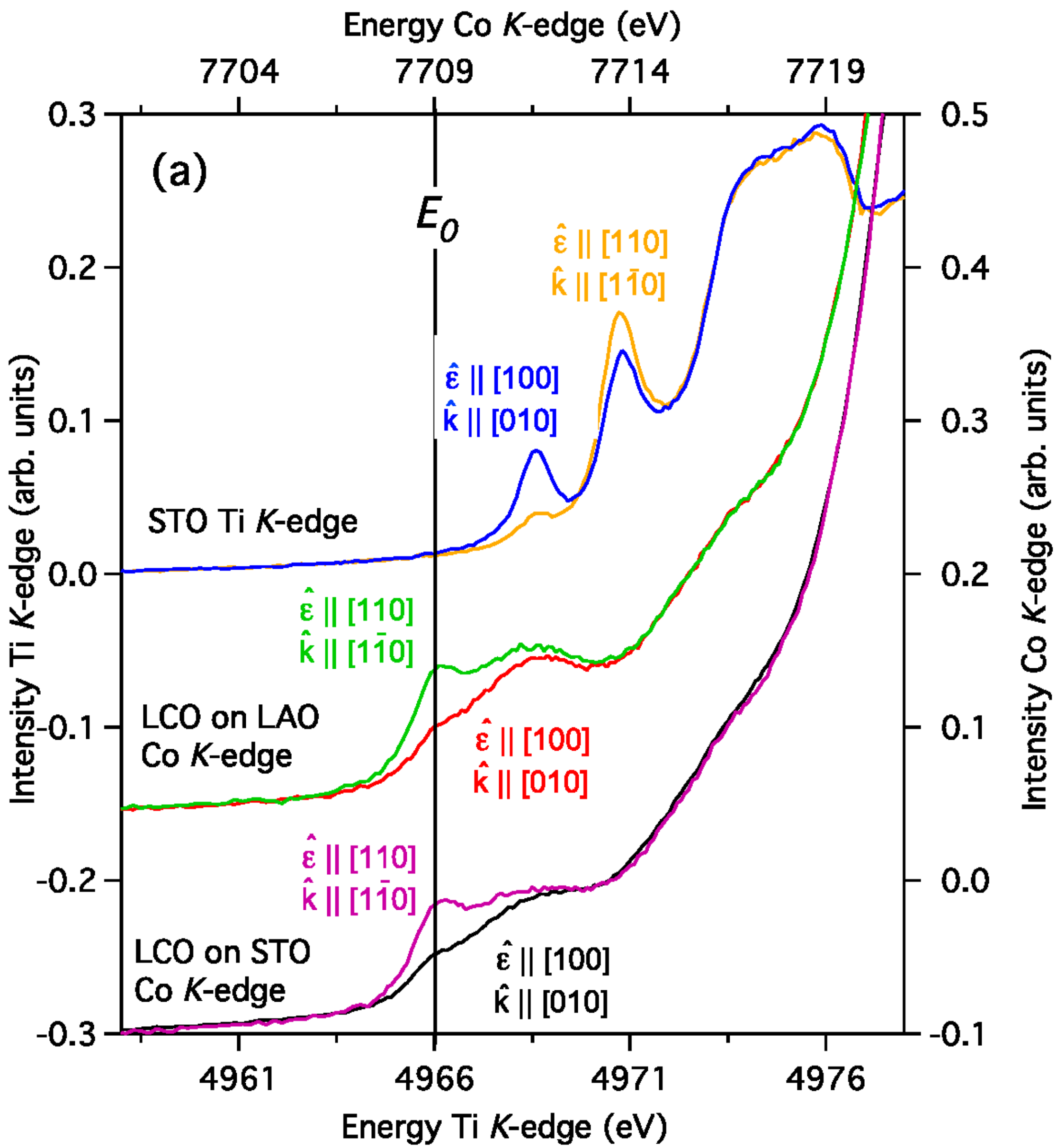

Energy Co K-edge (eV)
7704
7709
7714
7719
0.3
0.2
0.1
0.0
-0.1
-0.2
-0.3
0.5
0.4
0.3
0.2
0.1
0.0
-0.1
(a)
E0
ε̂ || [110]
k̂ || [11̄0]
ε̂ || [100]
k̂ || [010]
STO Ti K-edge
ε̂ || [110]
k̂ || [11̄0]
LCO on LAO
Co K-edge
ε̂ || [100]
k̂ || [010]
ε̂ || [110]
k̂ || [11̄0]
LCO on STO
Co K-edge
ε̂ || [100]
k̂ || [010]
4961
4966
4971
4976
Energy Ti K-edge (eV)
Intensity Ti K-edge (arb. units)
Intensity Co K-edge (arb. units)

Intersite 4*p*-3*d* hybridization in cobalt oxides: a resonant x-ray emission spectroscopy study

György Vankó,[1,2] Frank M. F. de Groot,[3] Simo Huotari,[2] R. J. Cava,[4] Thomas Lorenz,[5] and M. Reuther[5]
[1] *KFKI Research Institute for Particle and Nuclear Physics, P.O. Box 49, H-1525 Budapest, Hungary*
[2] *European Synchrotron Radiation Facility, B.P. 220 F-38043 Grenoble Cedex 9, France*
[3] *Inorganic Chemistry and Catalysis, Department of Chemistry, Utrecht University, Sorbonnelaan 16, 3584 CA Utrecht, Netherlands*
[4] *Department of Chemistry, Princeton University, Princeton, NJ 08544, USA*
[5] *II. Physikalisches Institut, Universität zu Köln, Zülpicher Strasse 77, 50937 Köln, Germany*
(Dated: February 20, 2008)

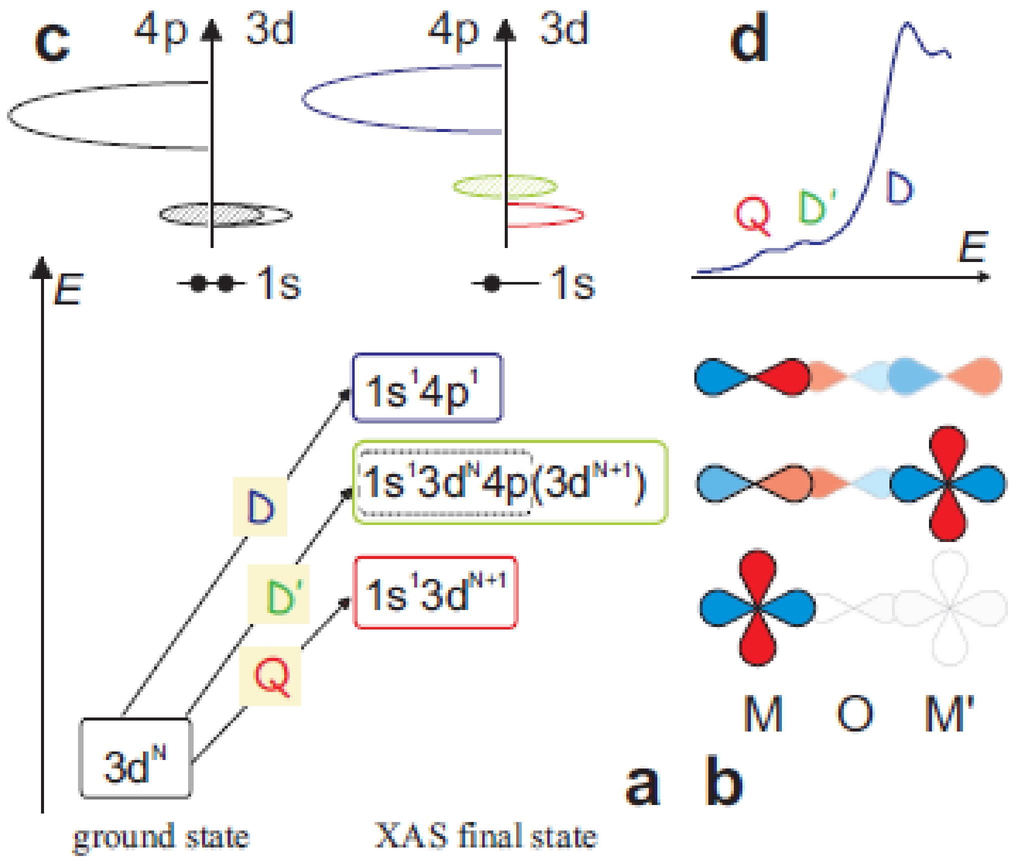

Polarization dependence of Ti K edge of cubic $SrTiO_3$

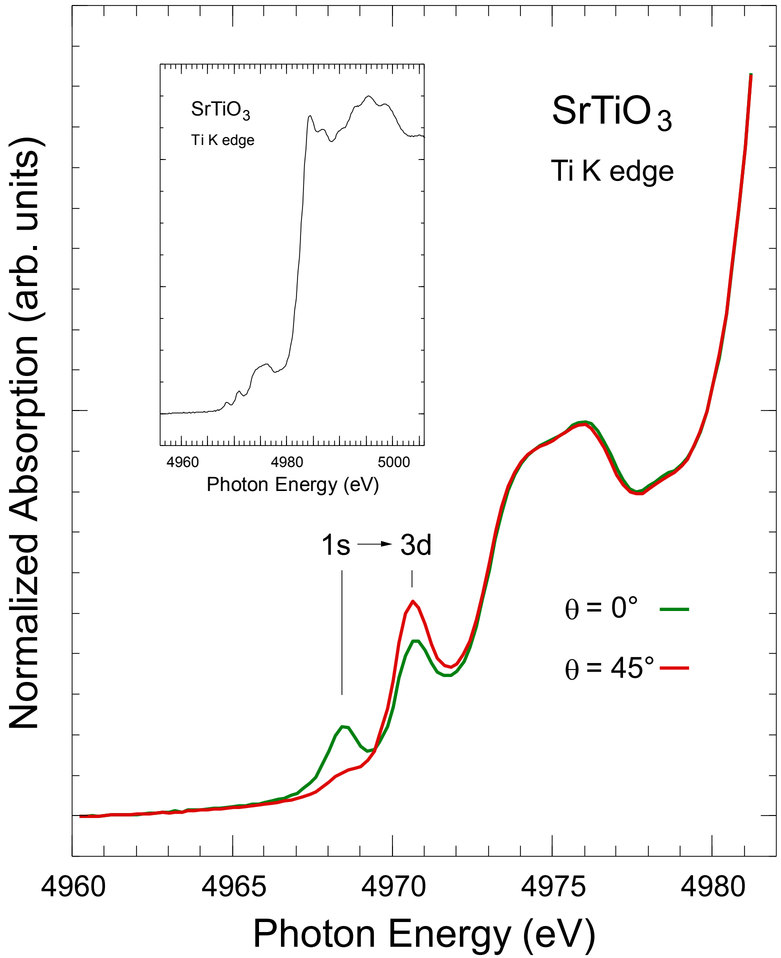

- Dipole: $\Delta l = \pm 1$

  $\sigma \propto |\langle f | \boldsymbol{\varepsilon}\cdot\mathbf{r} | i \rangle|^2$

  Ti 1*s* → 4*p*

- Quadrapole: $\Delta l = \pm 2$

  $\sigma \propto |\langle f | (\boldsymbol{\varepsilon}\cdot\mathbf{r})(\mathbf{k}\cdot\mathbf{r}) | i \rangle|^2$

  Ti 1*s* → 3*d*

Quadrupolar Transitions Evidenced by Resonant Auger Spectroscopy

J. Danger,[1,2,3] P. Le Fèvre,[1] H. Magnan,[1,2] D. Chandesris,[1] S. Bourgeois,[4] J. Jupille,[5] T. Eickhoff,[6] and W. Drube[7]

[1]*Laboratoire pour l'Utilisation du Rayonnement Electromagnétique, Université Paris Sud, Bâtiment 209d, BP 34, 91898 Orsay Cedex, France*

[2]*Service de Physique et de Chimie des Surfaces et des Interfaces, Commissariat à l'Energie Atomique, 91191 Gif-sur-Yvette Cedex, France*

[3]*Institut de Physique et de Chimie des Matériaux de Strasbourg, 23 rue du Loess, 67037 Strasbourg, France*

[4]*Laboratoire de Recherches sur la Réactivité des Solides, Université de Bourgogne, UFR Sciences et Techniques, 9 avenue Alain Savary, BP 47870, 21078 Dijon Cedex, France*

[5]*Laboratoire CNRS-Saint Gobain "Surface du Verre et Interfaces," 39 quai Lucien Lefranc, 93303 Aubervilliers, France*

[6]*Institut für Experimentalphysik, Universität Hamburg, Luruper Chaussee 149, 22761 Hamburg, Germany*

[7]*Hamburger Synchrotronstrahlungslabor HASYLAB, Deutsches Elektronen-Synchrotron DESY, Notkestraße 85, 22603 Hamburg, Germany*

(Received 25 June 2001; published 29 May 2002)

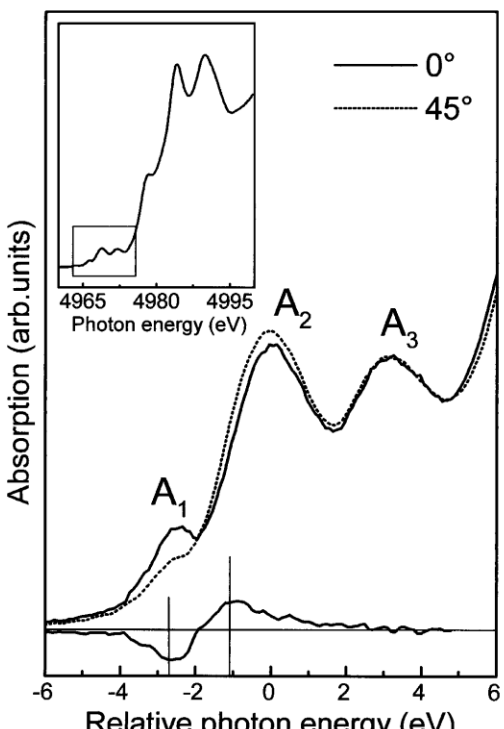

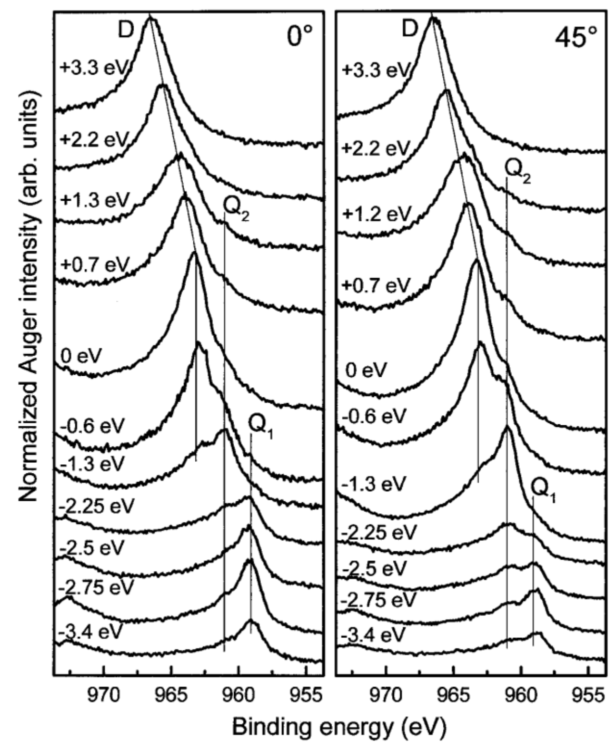

KLL around t_{2g}

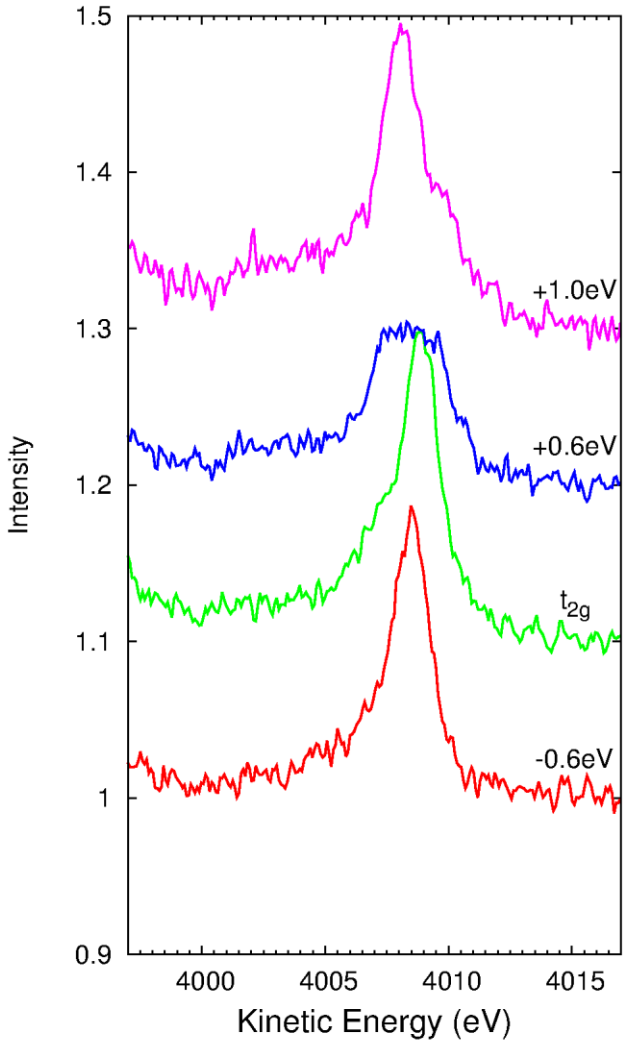

Main and spectator lines!

KLL around e_g

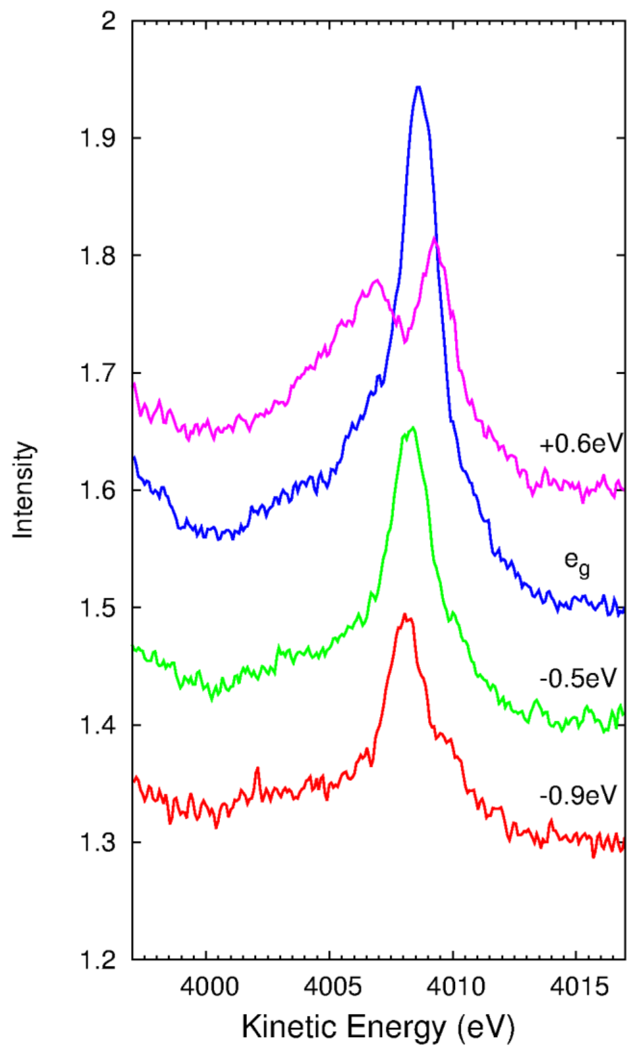

KLL around t_{2g}^* and e_g^*

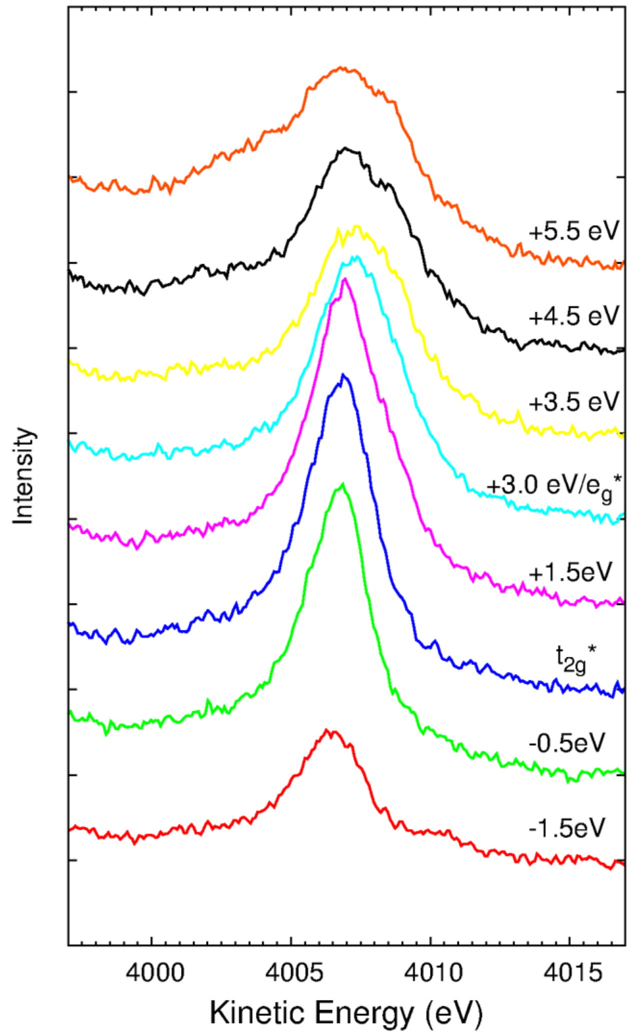

KLL around 4p (white line)

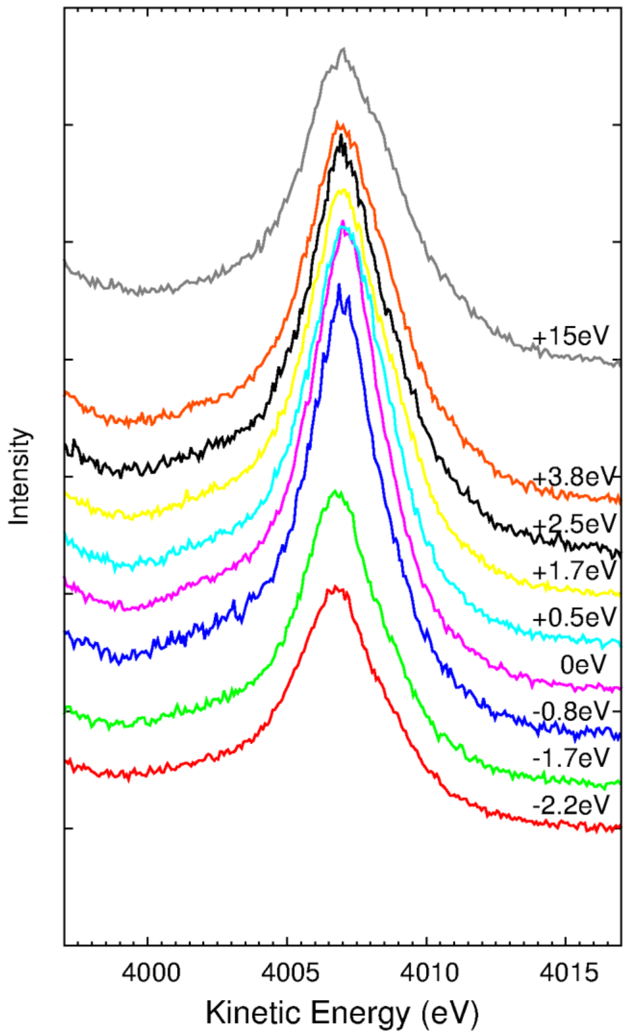

State-dependent screening (*l,E,r*)

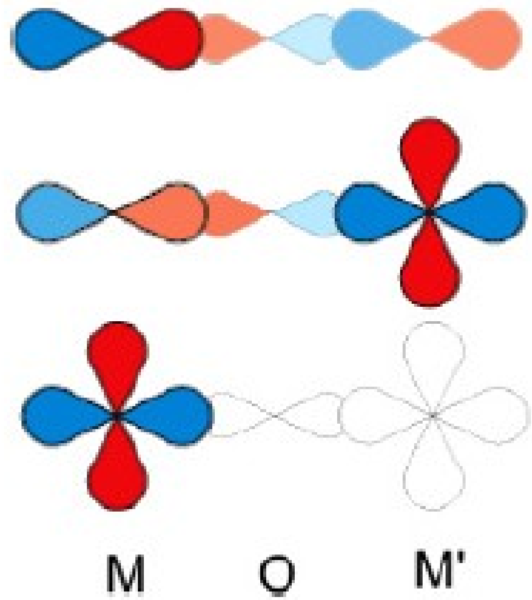

Figure 7. The final-state configurations of the 1s 4p dipole (top), the non-local 1s 4p(3d) dipole (middle) and the 1s 3d quadrupole (bottom) transitions.

KLL @ t_{2g}, t_{2g}^*, and 4p

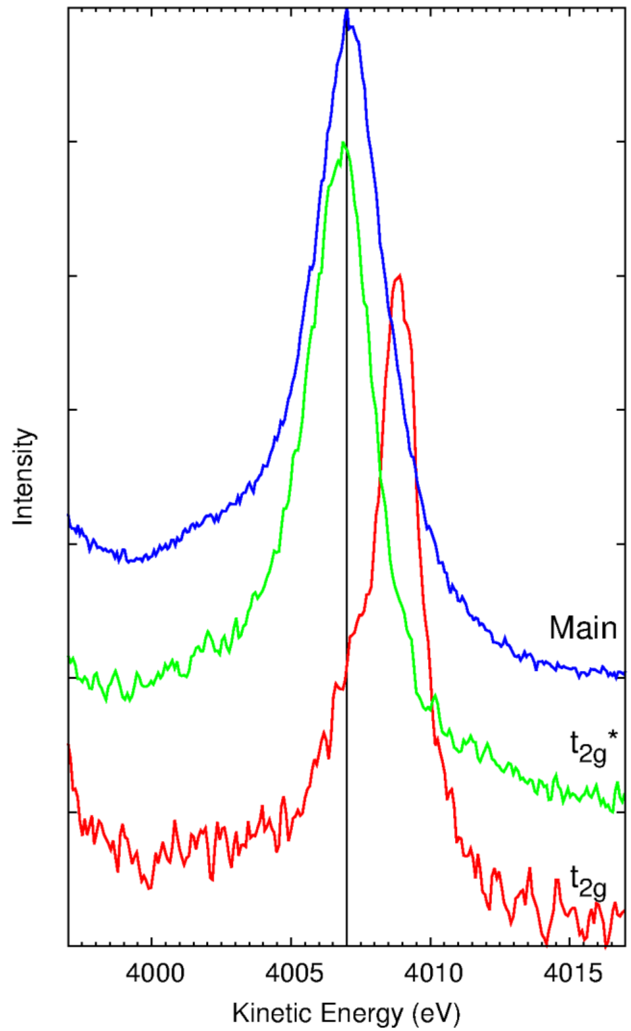

Collaborators

- Daniel Fischer (NIST)
- Barry Karlin (NIST)
- Conan Weiland (NIST)
- Johnny Kirkland (NIST)
- George Sterbinsky (NIST)
- Abdul Rumaiz (BNL)
- Joseph Lenhart (ARL)
- Michael Brumbach (Sandia)
- James Ohlhausen (Sandia)
- Kevin Zavadil (Sandia)
- Patrick Lysaght (SEMATECH)

Polarization dependence of Ti K edge of cubic and strained $SrTiO_3$

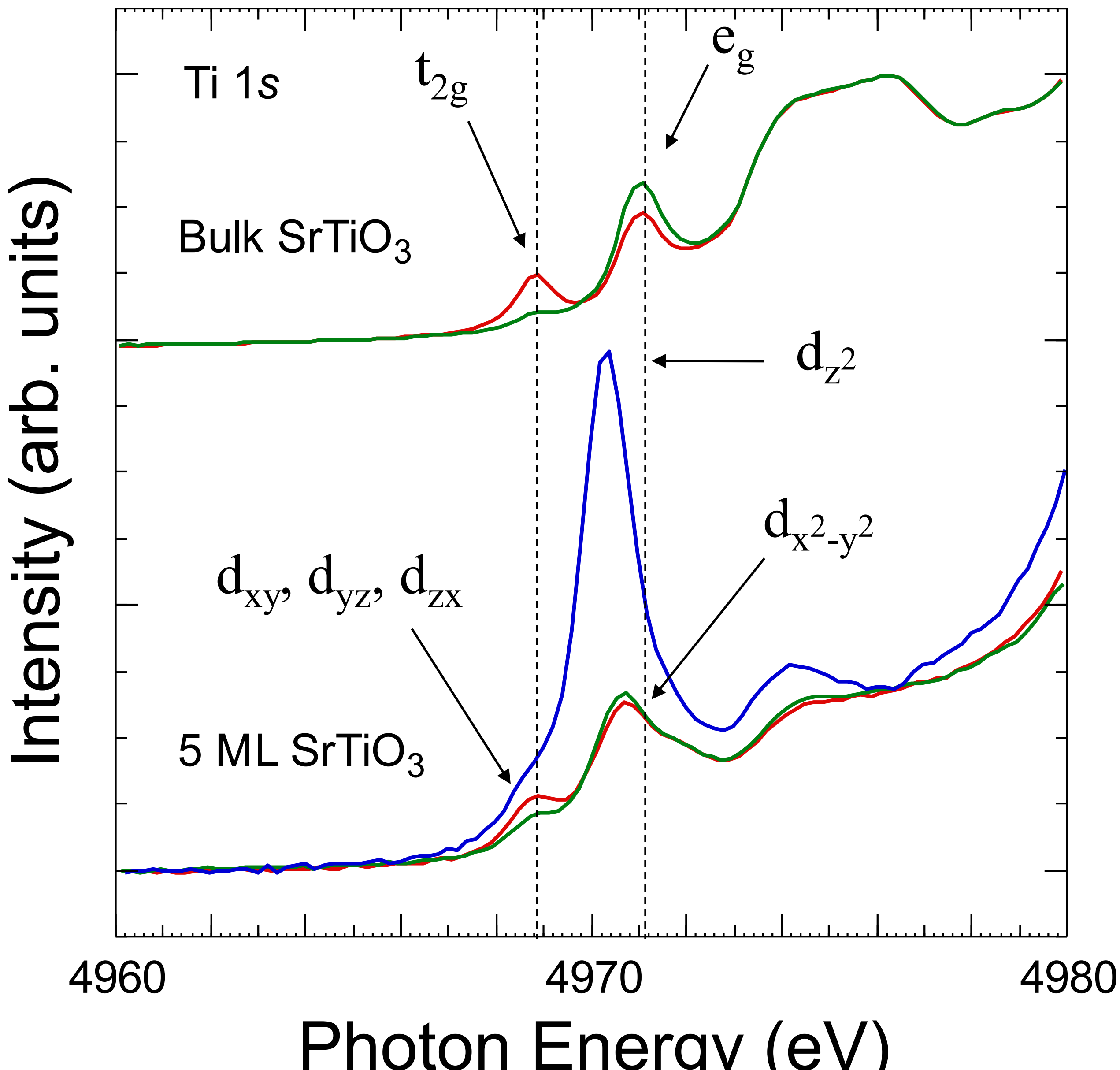

DFT Cubic and Strained $SrTiO_3$

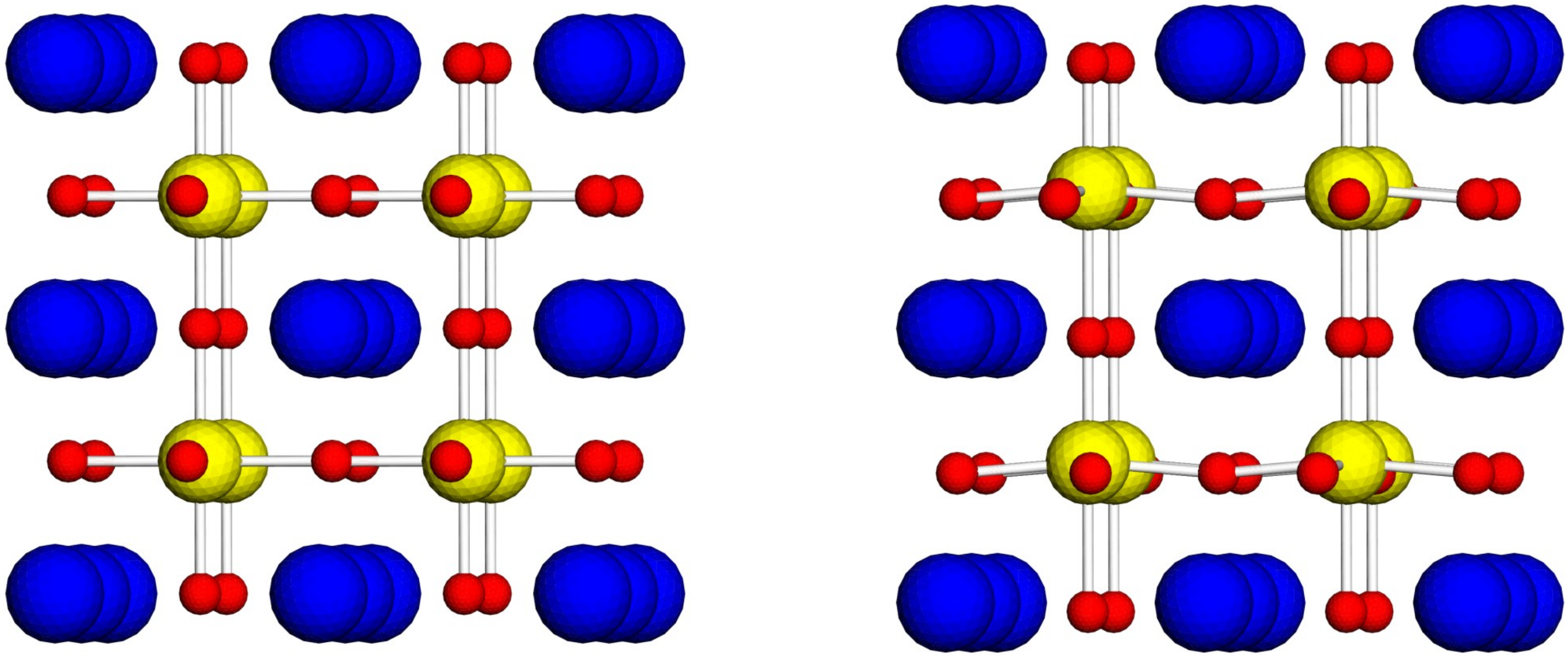

Bethe-Salpeter Calculations of Ti K edge XAFS

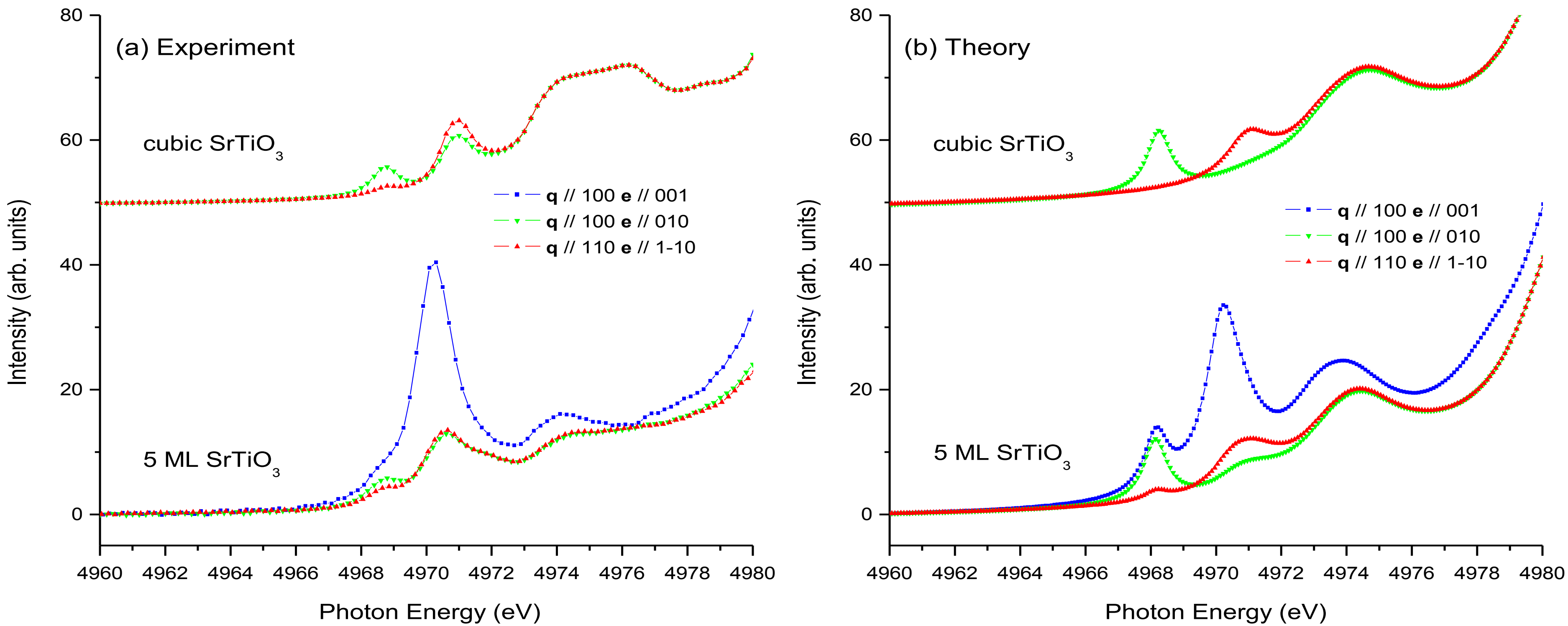

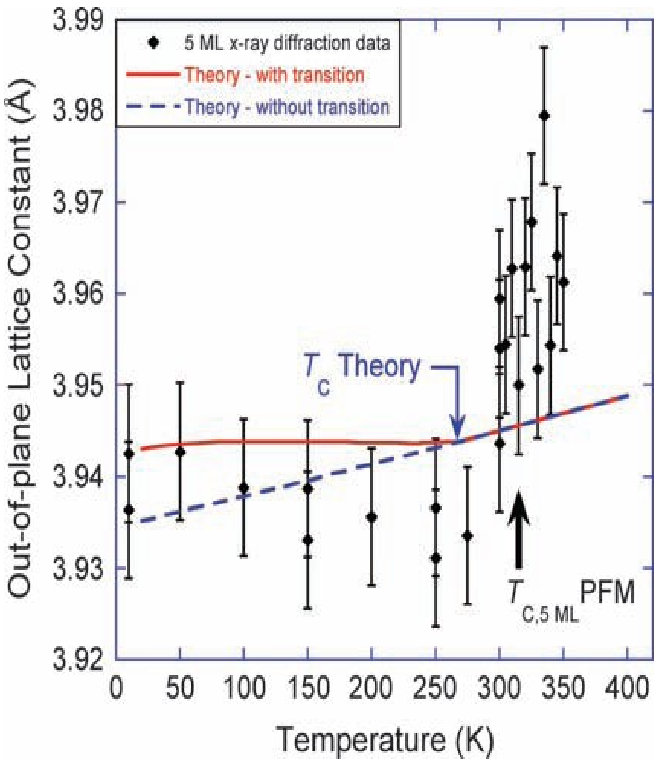

295K

Pattern written with 2V

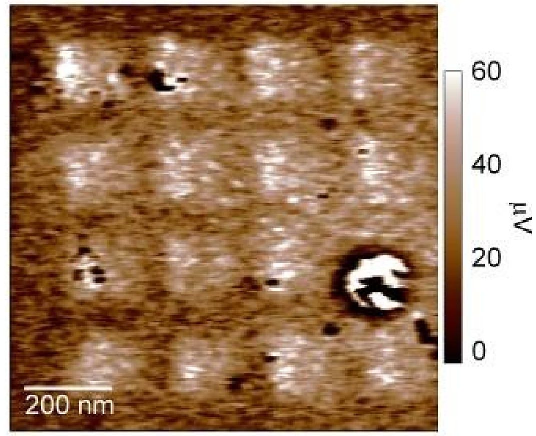

295K

Pattern written with -2V

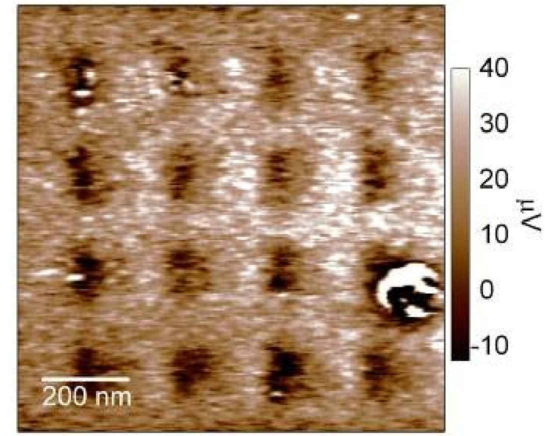

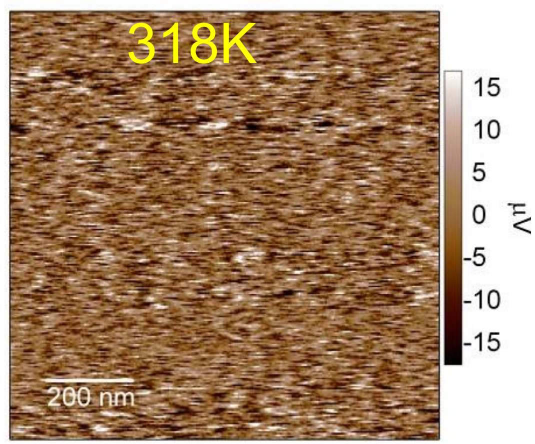

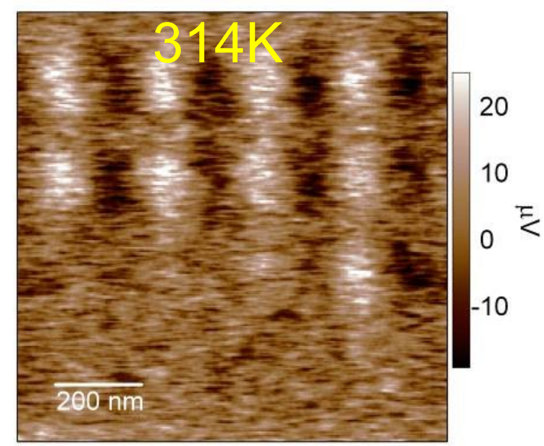

PHYSICAL REVIEW A VOLUME 50, NUMBER 2 AUGUST 1994

Threshold *K*-*LL* Auger spectra of P in InP

Honghong Wang,[1] Joseph C. Woicik,[2] Teijo Åberg,[3] Mau Hsiung Chen,[4] Alberto Herrera-Gomez,[5] Tom Kendelewicz,[5] Anna Mäntykenttä,[6] Ken E. Miyano,[7] Stephen Southworth,[8] and Bernd Crasemann[1]

[1]*Department of Physics, University of Oregon, Eugene, Oregon 97403*

[2]*Materials Science and Engineering Laboratory, National Institute of Standards and Technology, Gaithersburg, Maryland 20899*

[3]*Laboratory of Physics, Helsinki University of Technology, SF-02150 Espoo, Finland*

[4]*High-Temperature Physics Division, Lawrence Livermore National Laboratory, Livermore, California 94550*

[5]*Stanford Electronics Laboratories, Stanford University, Stanford, California 94305*

[6]*Department of Physics, University of Oulu, SF-90570 Oulu, Finland*

[7]*Department of Physics, Brooklyn College, Brooklyn, New York 11210*

[8]*Physics Laboratory, National Institute of Standards and Technology, Gaithersburg, Maryland 20899*

(Received 16 March 1994)

The evolution of K-$L_{2,3}L_{2,3}$ $^1D_2$ radiationless resonant Raman scattering into Auger-electron emission was studied by tuning synchrotron radiation across the K edge of P in InP. The spectrum can be interpreted in terms of a two-component model that involves excitation of a photoelectron (1) into a discrete excitonlike state and (2) into the continuum; extra-atomic relaxation is taken into account. Auxiliary studies of above-threshold Auger and photoelectron spectra arising from K photoionization were used to identify the dominantly atomic features of these spectra.

PACS number(s): 32.80.Hd, 32.80.Fb

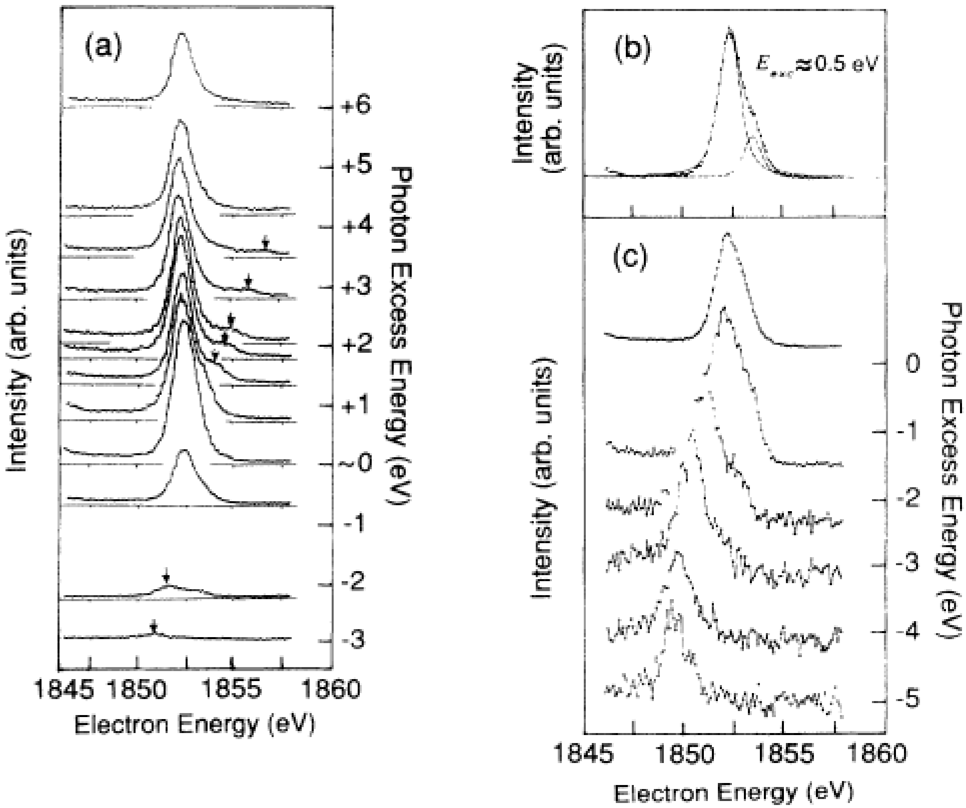

(a)
Intensity (arb. units)
Photon Excess Energy (eV)
+6
+5
+4
+3
+2
+1
~0
-1
-2
-3
1845
1850
1855
1860
Electron Energy (eV)
(b)
E_{exc}≈0.5 eV
Intensity (arb. units)
(c)
Intensity (arb. units)
Photon Excess Energy (eV)
0
-1
-2
-3
-4
-5
1845
1850
1855
1860
Electron Energy (eV)

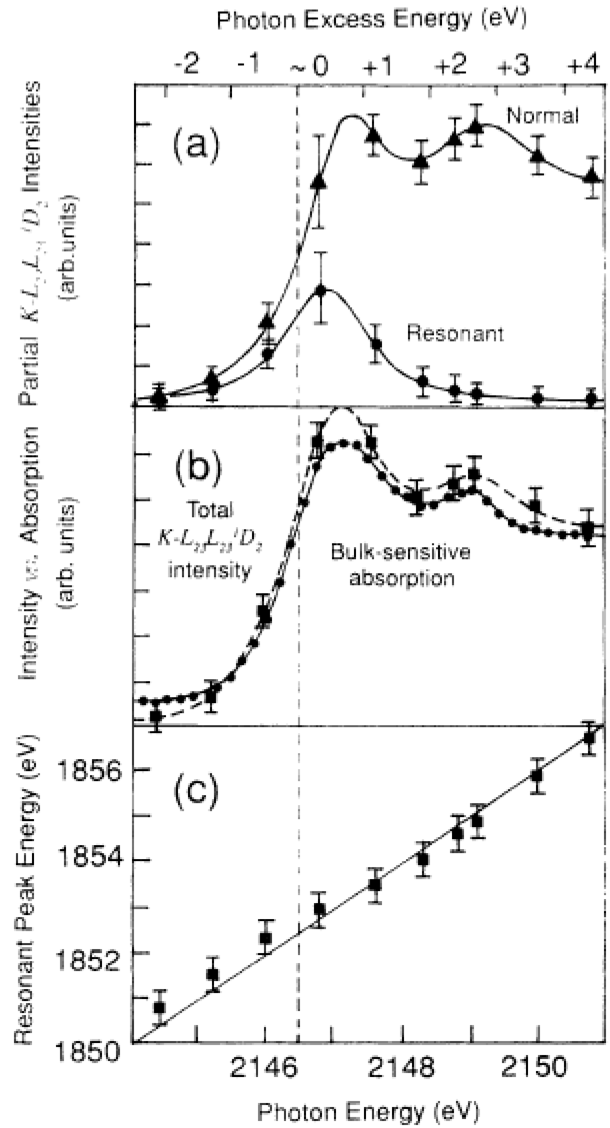

Photon Excess Energy (eV)
-2
-1
~0
+1
+2
+3
+4
Partial $K\text{-}L_{23}L_{23}\,{}^1D_2$ Intensities
(arb.units)
(a)
Normal
Resonant
Intensity vs. Absorption
(arb. units)
(b)
Total
$K\text{-}L_{23}L_{23}\,{}^1D_2$
intensity
Bulk-sensitive
absorption
Resonant Peak Energy (eV)
(c)
1856
1854
1852
1850
2146
2148
2150
Photon Energy (eV)